Load history effects on fracture toughness of RPV steel

Jérémy Hure*, Benoît Tanguy

CEA, DEN, Service d'Etudes des Matériaux Irradiés, 91191 Gif-sur-Yvette, France
* Corresponding author: Jeremy.hure@cea.fr

Abstract Fracture toughness is required for assessing structural integrity of reactor pressure vessels (RPV). However, it has been long recognized that load history effects can increase the apparent toughness, which is not considered in practical rules assessment. This could lead to over pessimistic assessment in case of thermomechanical transient. The so-called warm prestress (WPS) effect corresponds to the absence of crack propagation after prestressing if the load is held constant or decreased as the temperature is decreased. This study investigates the WPS effect on A508 Cl3 RPV steel, focusing on transient loadings in which the load is increased during cooling, with a twofold aim. Firstly to investigate experimentally to which extent it is possible to go beyond the WPS effect by progressively increasing the slope of the transient. Secondly, to assess numerically the ability of local approach to fracture (LAF) models to quantitatively predict the experimental results. The evolution of local quantities such as opening stress, cumulated plastic strain, triaxiality close to the crack tip are finally described in details.

Keywords Warm prestress effect, Cleavage fracture, RPV steel, Local approach to fracture

1. Introduction

The warm prestress (WPS) effect describes the fact that, when a crack is loaded at a temperature T_1 to a stress intensity factor K_1, no fracture will occur if the stress intensity factor decreases or is held constant between T_1 and $T_2 < T_1$, even if the fracture toughness of the virgin material (*i.e* without prior loading) is exceeded [1, 2]. The WPS effect has been the object of several experimental studies on ferritic steels (see e.g. [3]) as security assessment of nuclear reactor pressure vessels (RPV) requires to consider the case of a loss of coolant accident (LOCA) in which the vessel is subjected to a mechanical loading associated with a variation of the temperature. In this particular case, the embrittlement due to neutron irradiation has to be considered and, in the perspective of prolongation of nuclear power plant lifetime, the WPS effect has to be well understood in order to justify security margins. In this paper, we study the WPS effect on French RPV 16MND5 (similar to A508 Cl3) steel, focusing on transient loadings in which the load is increased while cooling the specimen (Fig. 1). Our aim is first, from an engineering point of view, to quantify how much it is possible to go beyond the conservative principle of WPS effect, *i.e.* no propagation if the load is held constant or decreased during cooling. Secondly, we use these WPS cycles to compare the numerical predictions of local approach to fracture (LAF) models, the differences being discussed by looking in details at the evolution of the crack tip stress/strain fields.

2. Experimental results

2.1 Mechanical tests

The material studied is a 16MND5 steel (similar to A508 Cl3 steel) that originates from a forged nozzle shell of a pressurized water reactor of 220 mm thickness [4]. CT specimens precracked at a ratio $a_0/W \sim 0.56$ (where a_0 is the fatigue precrack length and W the width) are tested using ASTM E1921 standard recommendations [5]. Isothermal fracture toughness tests were performed using specimens of two different thicknesses (B=12.5 and 25 mm), leading to a reference temperature, T_0, equal to -104.7°C [4].

WPS experiments presented in this study were performed using standard CT specimens with a 25 mm thickness. Four different types of WPS cycles were conducted: LCF (Load-Cool-Fracture), LCDKF (Load-Cool-Decreasing K-Fracture), LCIKF (Load-Cool-Increasing K-Fracture) and LCOIKF (Load-Cool-Oscillating Increasing K-Fracture) (Fig. 1). For all the WPS cycles, the loading sequence was: (i) Loading up to 500 N under displacement control with a crosshead speed of 0.25 mm/min, (ii) loading up to K_{WPS} under extensometer control at 0.1 mm/min, (iii) Cooling from T_{WPS} down to T_{frac} under load control with a temperature rate of -1.5°C/min, (iv) Reloading up to fracture under extensometer control at 0.1 mm/min if the specimen survived the transient. All values of K presented here, at WPS loading and fracture levels, are elastic values, thereafter noted K_{el}, calculated according to ASTM E 1921 [5].

2.1 Synthesis of the experimental data

The whole set of WPS experiments that were performed in this study are presented in Table 1. The first four cycles give us a reference base which will be useful for comparison to the main object of the study, LCIKF cycles. All specimens survived to the transient and failed during reloading phase. From all the WPS tests performed, the following observations can be made:

- LCF and LCDKF cycles performed on the 16MND5 RPV steel confirmed the numerous experimental results on ferritic steels published in the literature, *i.e.* no propagation if the load is held constant or decreased during cooling ;

- LCIKF cycles performed in this study confirm and extend the previous results [6, 7] that a critical slope has to be exceeded to induce cleavage during cooling.

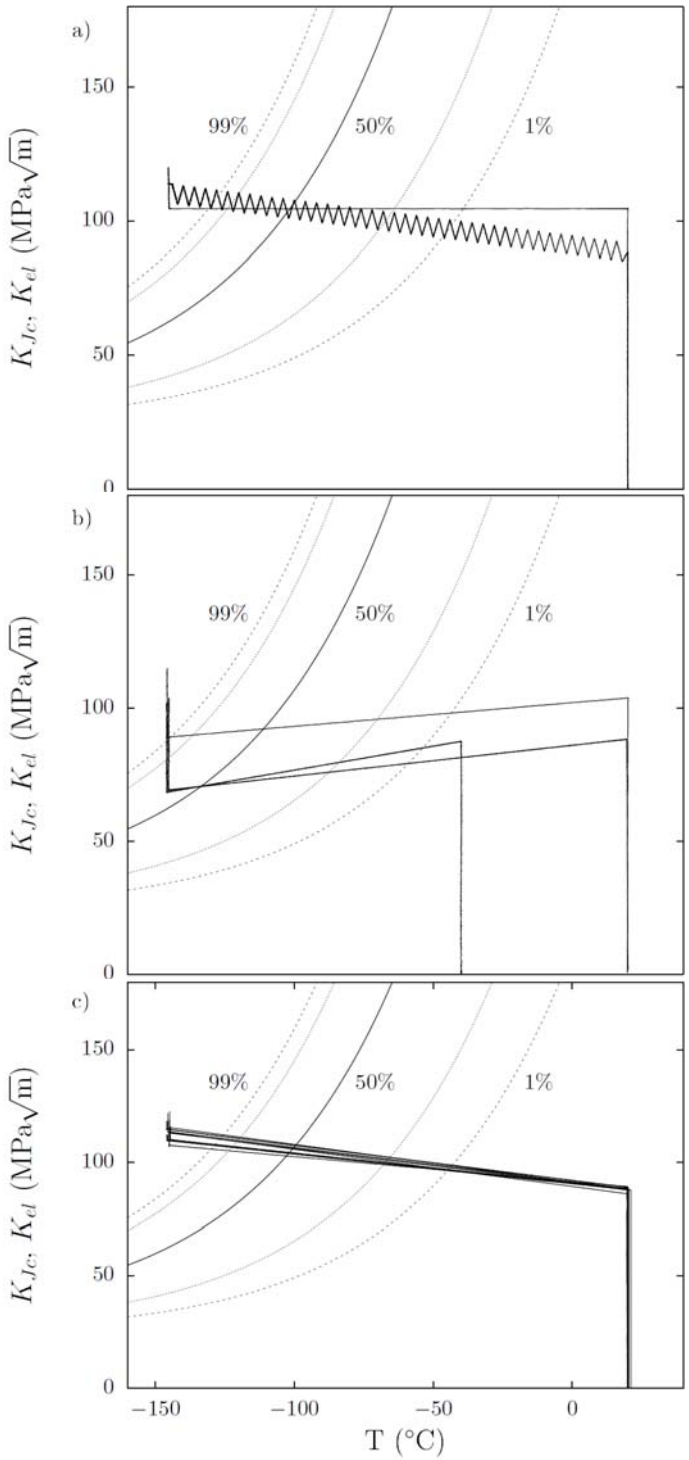

Figure 1 : Overview of all the transient loadings studied (LCF/LCOIKF (a), LCDKF (b), LCIKF (c)). Note that Master Curve confidence bounds are obtained considering elasto-plastic fracture toughness values, K_{Jc}, so that comparison with elastic values of stress intensity factors are not strictly valid.

No.	Cycle type	T_{WPS} (°C)	T_{frac} (°C)	K_{el}^{WPS} (MPa$\sqrt{\text{m}}$)	Targeted K_{el} (MPa$\sqrt{\text{m}}$)	$-\frac{\Delta K}{\Delta T}$ (MPa$\sqrt{\text{m}}$/°C)	K_{el}^{frac} (MPa$\sqrt{\text{m}}$)	$\frac{K^{frac}}{K^{WPS}}$	$\frac{K^{frac}}{K_{95\%}}$
H1ACT1	LCF	20.0	-145.2	104.6	-	-	114.3	1.09	1.40
H1ACT2	LCDKF1	20.0	-145.7	103.9	89.2	-0.089	114.8	1.10	1.41
H1ACT11	LCDKF2	19.6	-145.1	88.4	69.4	-0.115	103.8	1.17	1.27
H1ACT22	LCDKF3	-40.0	-145.9	87.5	68.5	-0.179	102.1	1.17	1.25
H1ACT16	LCIKF1	19.8	-144.9	89.2	107.6	0.112	114.7	1.29	1.41
H1ACT14	LCIKF2	20.0	-144.6	88.3	110.2	0.133	115.6	1.31	1.42
H1ACT5	LCIKF2	20.0	-145.0	87.9	109.7	0.132	112.1	1.28	1.37
H1ACT20	LCIKF3	20.0	-145.7	89.0	114.8	0.156	118.1	1.33	1.45
H1ACT41	LCIKF3	20.4	-145.0	88.2	113.6	0.154	119.0	1.35	1.44
H1ACT40	LCIKF3	19.9	-145.6	87.8	113.2	0.153	120.9	1.39	1.49
H1ACT27	LCIKF4	20.3	-145.1	86.0	113.3	0.165	117.9	1.37	1.44
H1ACT26	LCIKF4	21.1	-144.9	87.8	115.5	0.167	122.6	1.40	1.50
H1ACT15	LCOIKF*	20.0	-145.2	88.3	113.8	0.133	119.8	1.36	1.47

Table 1 : Experimental results on CT specimens are given for the various WPS cycles. * For LCOIKF cycle, the mean slope ΔK/ ΔT is given.

3. Numerical modeling

3.1 Local approach to fracture

As the local approach to fracture needs an accurate description of the stress/strain fields at the crack tip, the mechanical behavior of the material has to be modeled as precisely as possible, as well as the evolution of the characteristics with temperature. Large plastic deformations occur during the pre-loading at the crack tip, producing work-hardening so that finite strain formalism was used. Thus, elasto-visco-plastic constitutive equations were used in order to describe accurately the behavior of the material [8]:

$$\frac{1}{\dot{p}} = \frac{1}{\dot{p}_1} + \frac{1}{\dot{p}_2} \qquad \dot{p}_i = \left\langle \frac{f(\sigma,p)}{k_i} \right\rangle^{n_i}$$

$$f(\sigma,p) = \sqrt{\frac{3}{2}\underline{\underline{s}} : \underline{\underline{s}}} - R(p) \qquad R(p) = R_0 + Q_1(1-e^{-b_1 p}) + Q_2(1-e^{-b_2 p})$$

where p is the cumulated plastic strain, s the stress deviator and f(σ,p) the yield surface. The parameters determined in previous studies [4,9] are given in Table 2 and allow reproducing accurately both smooth tensile and notched tensile tests up to plastic strains of about 40% (Fig. 3).

	20°C	-50°C	-100°C	-150°C
E (MPa)	195224	203540	209480	215420
R_0 (MPa)	430.7	463.5	522.2	650.8
Q_1 (MPa)	167.9	203.1	228.3	253.5
b_1	26.8	19.1	13.6	10.1
k_1 (MPa s^{1/n_1})	31.25	62.05	84.05	84.05
n_1	5.18	6.24	6.99	6.99
Q_2 (MPa)	295.8			
b_2	3.5			
k_2 (MPa s^{1/n_2})	0.185			
n_2	1.15			
ν	0.3			

Table 2 : Young's modulus, Poisson's ratio and visco-plastic coefficients for 16MND5 steel

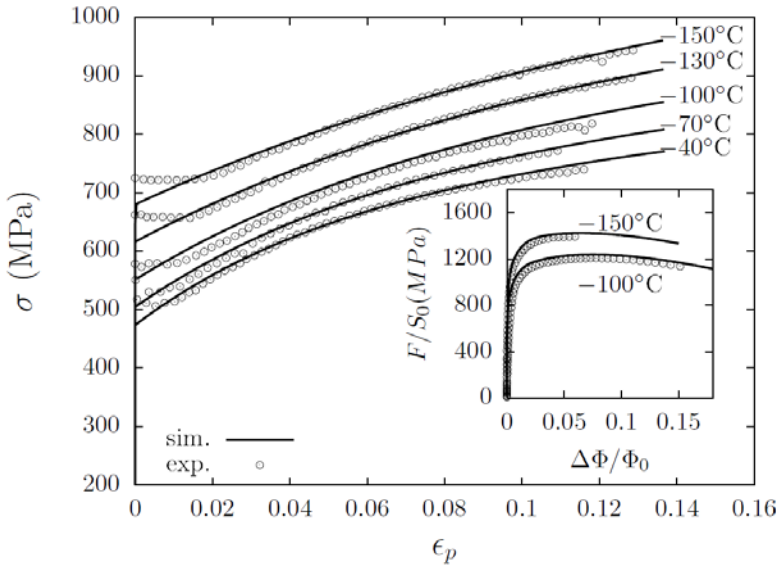

Figure 2 : Tensile curves at different temperature for 16MND5 steel. Open symbols correspond to the experimental data, solid lines to the modeling. Inset: Applied force vs. diameter reduction for AE notched specimens (notch radius 0.6mm, initial diameter φ_0=6mm). All the mechanical tests correspond to a strain rate of $\varepsilon = 5.10^{-4}s^{-1}$.

All the analysis were performed using the finite element software Cast3m [10] using the elasto-visco-plastic constitutive equations described above. CT specimens are modeled with 2D plane strain, quadratic, full integration elements.

Two different LAF models were used to predict the probabilities of cleavage fracture. The first one is the seminal Beremin model [11] modified to account for non-monotonic loadings [12]. The second is a simplified version of the model proposed by Bordet [6,13] which has the particularity to account explicitly for the necessity of active plasticity to trigger cleavage. The fracture probability for both models can be written as:

$$P_f = 1 - \exp\left(-\int_V \max_{t' \leq t, \dot{p}(t')>0, \sigma_I(t')>0} \left(\frac{\sigma_I(t')}{\sigma_u(t')}\right)^m \frac{dV}{V_0}\right)$$

$$P_f = 1 - \exp\left(-\left\{\int_V \left(\int_0^{\epsilon_p(t)} \frac{\sigma_Y}{\sigma_{Y,0}} \max\left(\frac{\sigma_I^m}{\sigma_u^m}, 0\right) d\epsilon_p\right) \frac{dV}{V_0}\right\}\right)$$

where σ_I is the largest principal stress and σ_Y the yield stress. In both models, the normalization volume V_0 is taken to be $0.001mm^3$, and in the Bordet model, the reference yield stress $\sigma_{Y,0}$ = 650MPa. The parameters σ_u and m have to be determined independently for each model to reproduce the experimental results of fracture toughness without prestressing. A F.E. simulation of a CT specimen was performed at -150°C, and the Beremin and Bordet models parameters were fitted so as to reproduce the fracture probability given by the Master Curve approach (with a reference temperature T_0 = -104.7°C). The parameters obtained are given below:

$$\sigma_{u,\mathrm{Beremin}} = 2575\mathrm{MPa} \qquad m_{\mathrm{Beremin}} = 25$$
$$\sigma_{u,\mathrm{Bordet}} = 2065\mathrm{MPa} \qquad m_{\mathrm{Bordet}} = 21$$

As shown in [8,14], for this steel a constant value of σ_u can be used only on a typical range [-150:-50°C], higher values being needed at higher temperatures. However, for the LCIKF cycles where cleavage is potentially expected, the loading path is under the Master Curve for T>-50°C (see Fig. 1), so that no cleavage fracture is expected. The temperature dependence of σ_u is thus not considered here. For practical reasons, when post-processing the simulations, the value of σ_u is taken as constant in the range [-150:-50°C], and to a very high value above. The results from LAF models - corresponding to probability of failure of 5%, 50% and 95% - and their comparisons with experimental data are shown in Fig. 3.

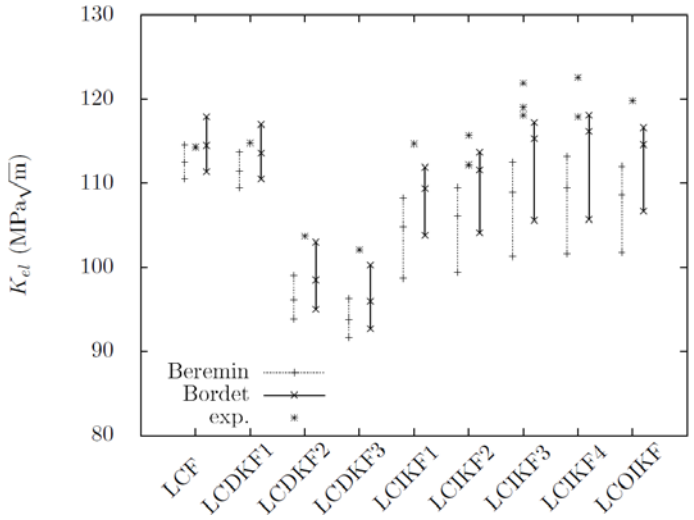

Figure 3 : Elastic stress intensity factor K_{el} at fracture for the different WPS cycles. Dots correspond to the experimental data, dashed and solid lines to the fracture probability of 5%, 50% and 95% for Beremin and Bordet models, respectively.

Several observations can be made from the comparison in Fig. 3:

- For the LCF and LCDKF cycles, both models give predictions in good agreement with experimental data, Bordet model being less conservative than the Beremin model.

- For LCIKF cycles, both models underestimate the toughness after warm prestressing, but predictions from Bordet model are closer to the experimental data.

- For all transient loadings, the scatter after warm prestressing is larger for Bordet model than for Beremin model.

These results tend to indicate that, after warm prestressing, the simplified version of the model proposed by Bordet gives more accurate predictions than the Beremin model which is more conservative. To better understand and assess the physical hypothesis used in the models – and thus why do they lead to slightly different results - the evolution of mechanical quantities such as plastic zone size and stress/strain fields during the WPS cycles are investigated in more details in the following section.

3.2 Evolution of local parameters

The basic assumption for the WPS effect to happen is that the size of the plastic zone at reloading is much smaller than the one at preloading. In other words, this means that the material keeps the memory of the prestressing at high temperature. Conversely, if the size of the plastic zone when reloading is much larger than the one at preloading, no WPS effect is expected. The evolution of the size of the active plastic zone as a function of the temperature is shown in Fig. 4 for LCIKF cycles. The size is normalized by the square of the thickness B^2, which confirms the plane strain assumption. For all the transient, the size is roughly constant up to a temperature of about -75°C, and then decreases drastically. In the temperature range where the size of the plastic zone is large, the path is under the Master Curve, thus no cleavage is expected. When the paths goes through the Master Curve and above, plasticity is almost not active - except on a very small area close to the crack tip - which explains roughly why cleavage fracture was not observed for the LCIKF cycles. Note that the evolution of the active plastic zone size could have been guessed without F.E. simulations: under small scale yielding assumption plastic zone extent scales as $(K/\sigma_Y)^2$ and K increases linearly with temperature in LCIKF experiments, while σ_Y increases exponentially.

Beremin and Bordet models both account for active plasticity, by integrating Weibull stress on the active plastic zone for the former, by considering nucleation of microcracks that depends on plastic strain for the latter so that the models will not predict cleavage fracture during the studied transients.

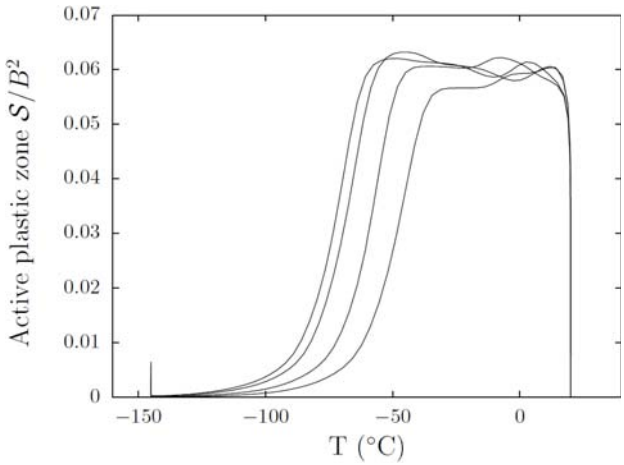

Figure 4 : Evolution of the active plastic zone for LCIKF cycles.

The history of local mechanical parameters - principal stress σ_I, cumulated plastic strain p and triaxiality τ - at the physical point where cleavage is triggered (identified by SEM investigations) were computed for each specimen. The results corresponding to the different experiments are shown in Fig. 5 where circles indicate cleavage fracture. The case of an isothermal test was added in Fig. 5 for comparison.

For all the experiments, the maximum principal stress and the cumulated plastic strain are increasing at cleavage triggering. This is consistent with the hypotheses of Beremin type models that consider the necessity of plastic flow to initiate microcracks and a stress-controlled propagation. Moreover, we note that the value of principal stress at which the cleavage fracture is triggered is almost the same for all the experiments (with or without warm prestressing), about 2250MPa, whatever the level of plastic strain, reinforcing the idea of a critical stress needed to propagate cracks. Note that this value of critical stress is higher than the one found in [4], as our modeling slightly overestimates stresses at large strains (see inset fig. 3). Compared to the isothermal test, the plastic strain at fracture - and its evolution with stress - is larger for WPS tests. The evolution of the triaxiality *vs.* stress is also different for WPS tests than for isothermal tests, which suggests that LAF models should include the effect of triaxiality.

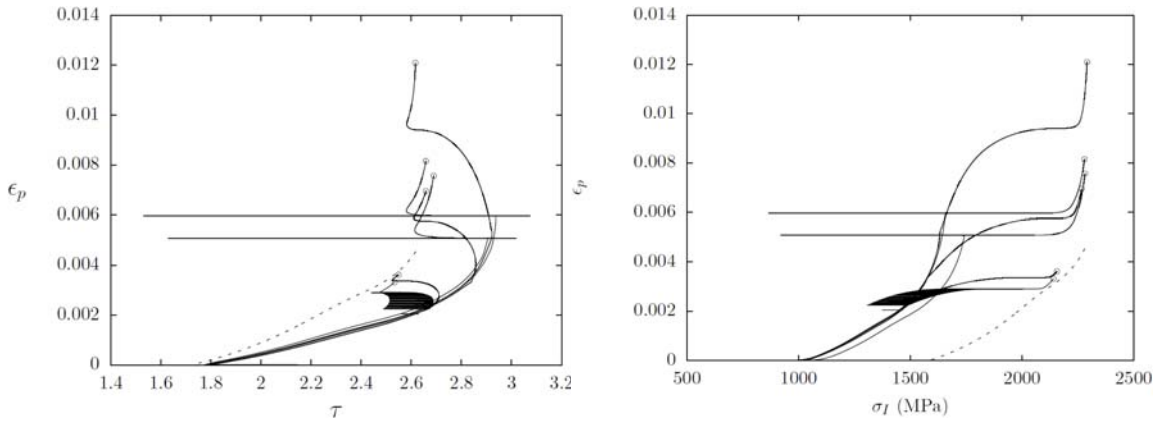

Figure 5: Evolution of plastic strain as a function of the principal stress (b) and triaxiality (b) at the location where cleavage was found to be triggered from microstructural investigations. Solid lines correspond to WPS experiments, dashed lines to isothermal test at -150°C.

Results from Fig. 5, and especially the different levels of plastic strains for a given stress that can be achieved in WPS experiments compared to isothermal tests, suggest that integrating over the active plastic zone may not be enough to account for the necessity of plastic strains. This may explain why considering strain-controlled germination of microcracks as in the Bordet model leads to better estimate of fracture toughness after prestressing.

4. Conclusion

In this study, the warm prestress effect on 16MND5 RPV steel was studied, focusing on transient loadings in which the load increases during cooling. The existence of a critical slope under which no propagation occurred is confirmed for this steel. Looking at the evolution of the active plastic zone gives some insights into the physical explanation of this critical slope: in the last part of the transient where the loading path is above the Master Curve, plasticity is confined to the vicinity of the crack tip and is much smaller than the size of the plastic zone at prestressing. Local approach to fracture models give predictions in good agreement with experimental data, a simplified version of the model proposed by Bordet *et. al.* leading to more accurate predictions The difference between the two models investigated is explained by looking at the evolution of stress, strain and triaxiality close to the crack tip: compared to an isothermal test, cumulated plastic strain can be larger for a given stress for WPS tests, suggesting that accounting explicitly for the necessity of plastic strain – as in the Bordet model – is required.

Acknowledgements

Financial and technical supports from CEA program RSTB and project MASOL is acknowledged. B. T. would like to thank P. Wident from SRMA/LC2M and his Master students N. Mozzani and J. Li who have been involved in this research project.

References

[1] B. Pickles, A. Cowan, A review of warm pre-stressing studies. Int. J. Pres. Ves. And Piping, 14 (1983) 95-131
[2] D. Smith, S. Garwood, The significance of prior overload on fracture resistance: A critical review. Int. J. Pres. Ves. And Piping, 41 (1990) 225-296
[3] K. Wallin, Master Curve implementation of the warm pre-stress effect. Eng. Fract. Mech. 70 (2003) 2587-2602
[4] B. Tanguy, C. Bouchet, S.R. Bordet, J. Besson, A. Pineau, Toward a better understanding of the cleavage in RPV steels: Local mechanical conditions and evaluation of a nucleation enriched Weibull model and of the Beremin model over a large temperature range. In 9th European Mechanics of Materials Conference, Local approach to fracture, Moret-sur-Loing (2006)
[5] ASTM E 1921- Standard test method for determination of reference temperature T_0 for ferritic steels in the transition range
[6] S. Bordet, B. Tanguy, J. Besson, S. Bugat, D. Moinereau, A. Pineau, Cleavage fracture of RPV steel following warm-prestressing: micromechanical analysis and interpretation through a new model. Fatigue Fract. Engng. Mater. Struct. 29 (2006) 799-816
[7] T. Yuritzinn, L. Ferry, S. Chapuliot, P. Mongabure, D. Moinereau, A. Dahl, Illustration of the WPS benefit through batman test series: Tests on large specimens under WPS loading

configurations. Eng. Fract. Mech 75 (2008) 2191-2207
[8] B. Tanguy, J. Besson, R. Piques, A. Pineau, Ductile to brittle transition of A508 steel characterized by Charpy impact test: Part II: modeling of the Charpy transition curve. Eng. Fract. Mech, 72 (2005) 413-434
[9] C. Bouchet, B. Tanguy, J. Besson, A. Pineau and S. Bugat, "Transferability of cleavage fracture parameters between notched and cracked geometries", The 16th European conference of fracture, Failure analysis of Nano and Engineering Materials and Structures, Alexandroupolis, July, 3-7, (2006)
[10] Cast3m DEN/DANS/DM2S
[11] F.M. Beremin, A local criterion for cleavage fracture of a nuclear pressure vessel steel. J. Metall. Trans. A 14A (1983) 2277-2287
[12] W. Lefevre, G. Barbier, R. Masson, G. Rousselier, A modified beremin model to simulate the warm pre-stress effect. Nucl. Eng. Design 216 (2002) 27-42
[13] S. Bordet, A. Karstensen, D. Knowles, C. Wiesner, A new statistical local criterion for cleavage fracture in steel Part I: Model presentation. Eng. Fract. Mech 72 (2005) 435-452
[14] B. Tanguy, C. Bouchet, S. Bugat, J. Besson , Local approach to fracture based prediction of the ΔT_{56J} and $\Delta T_{Kic,100}$ shifts due to irradiation for an A508 pressure vessel steel, Eng. Fract. Mech., 73, (2006), 191-206